Supporting Information

Self-assembly of Sb_2S_3 NRs-M (M=Au, Ag, Pd) Heterostructures Towards Boosted Photocatalysis

Huawei Xie,[a#] Bei-Bei Zhang,[b#] Fang-Xing Xiao* [b]

a. Department of Forensic Science, Fujian Police College, Fuzhou, China. The Engineering Research Center, Fujian Police College, Fuzhou, China.

b. College of Materials Science and Engineering, Fuzhou University, New Campus, Minhou, Fujian Province, 350108, China.

#These two authors contributed equally to this work.

E-mail: fxxiao@fzu.edu.cn

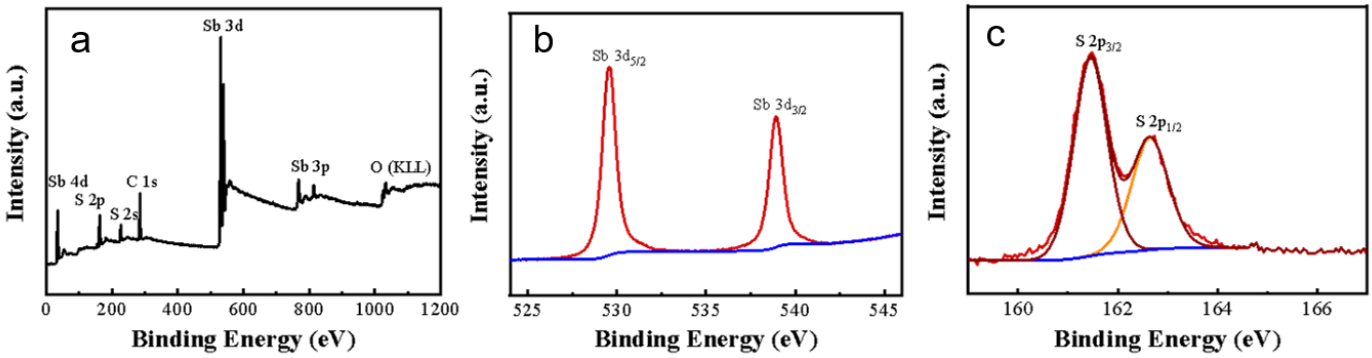

Fig. S1. (a) Survey and high-resolution (b) Sb 3d and (c) S 2p spectra of Sb_2S_3 NRs.

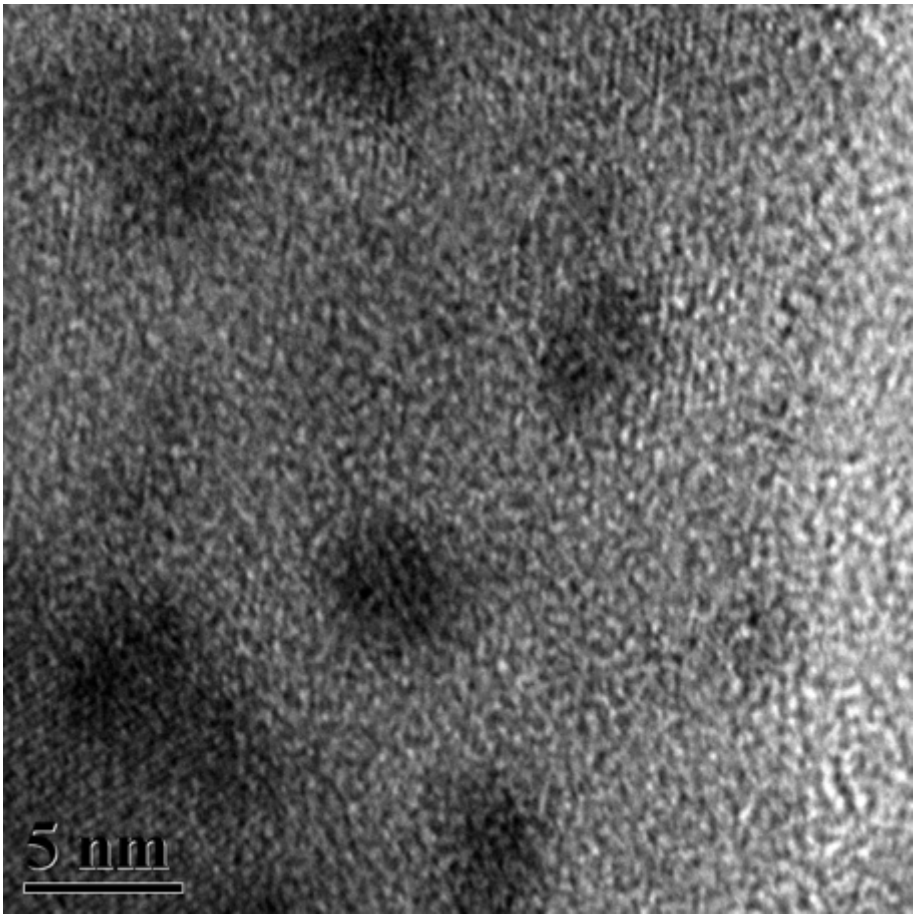

Fig. S2. HRTEM image of Sb_2S_3 NRs-2%Au heterostructure.

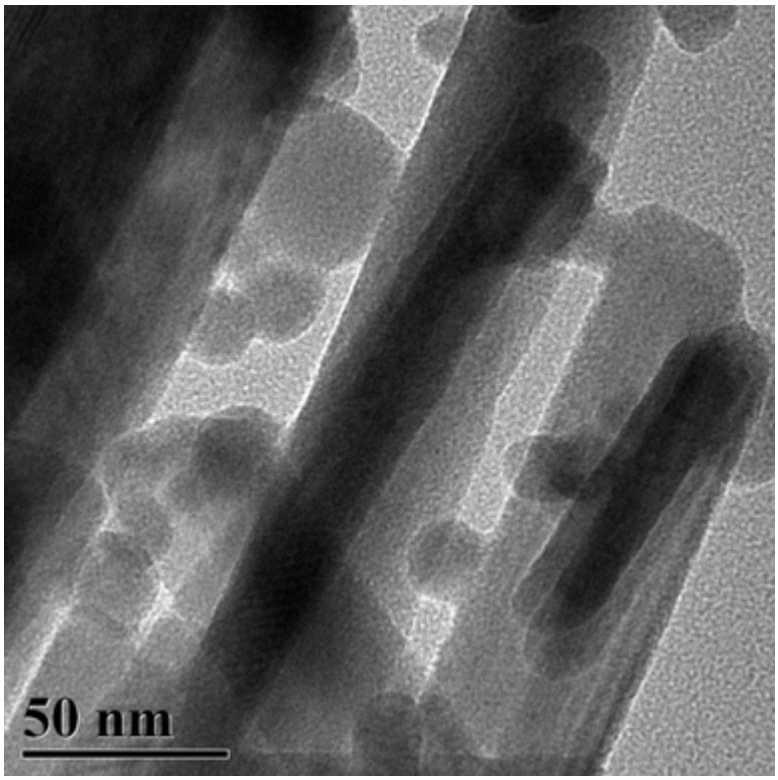

Fig. S3. TEM image of Sb_2S_3 NRs-3%Ag heterostructure.

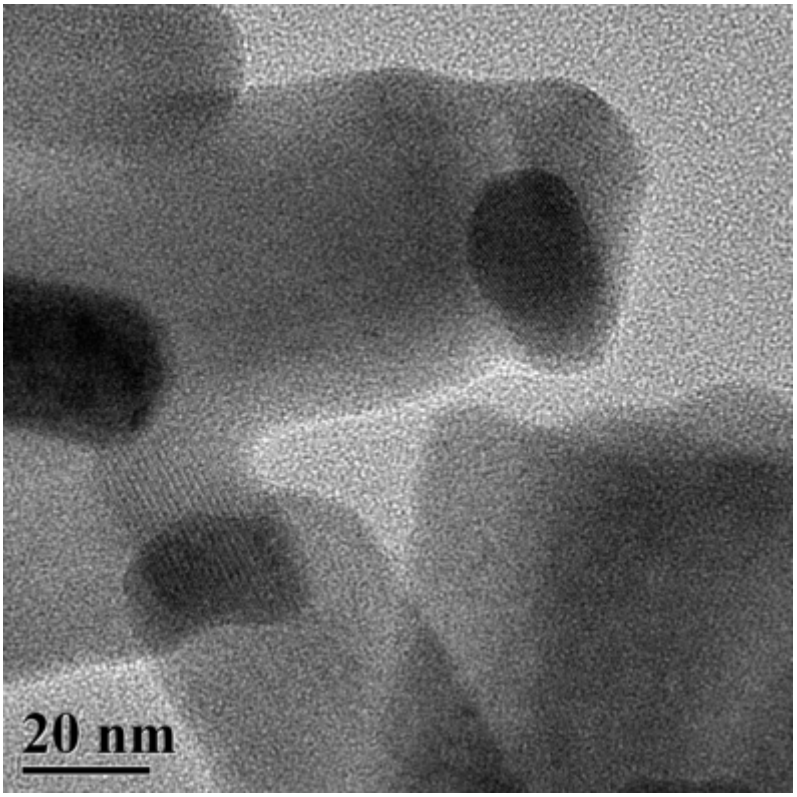

Fig. S4. TEM image of Sb_2S_3 NRs-2%Pd heterostructure.

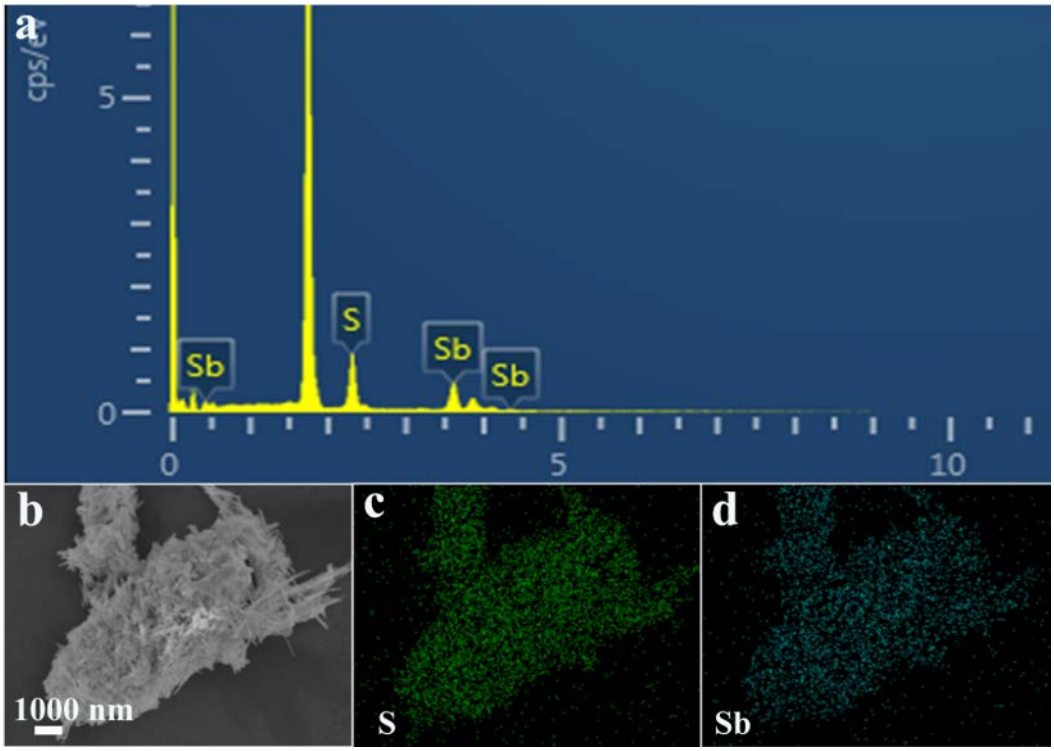

Fig. S5. (a) SEM image and (e) EDX result of Sb_2S_3 NRs with elemental mapping results for (b) Sb and (c) S signals.

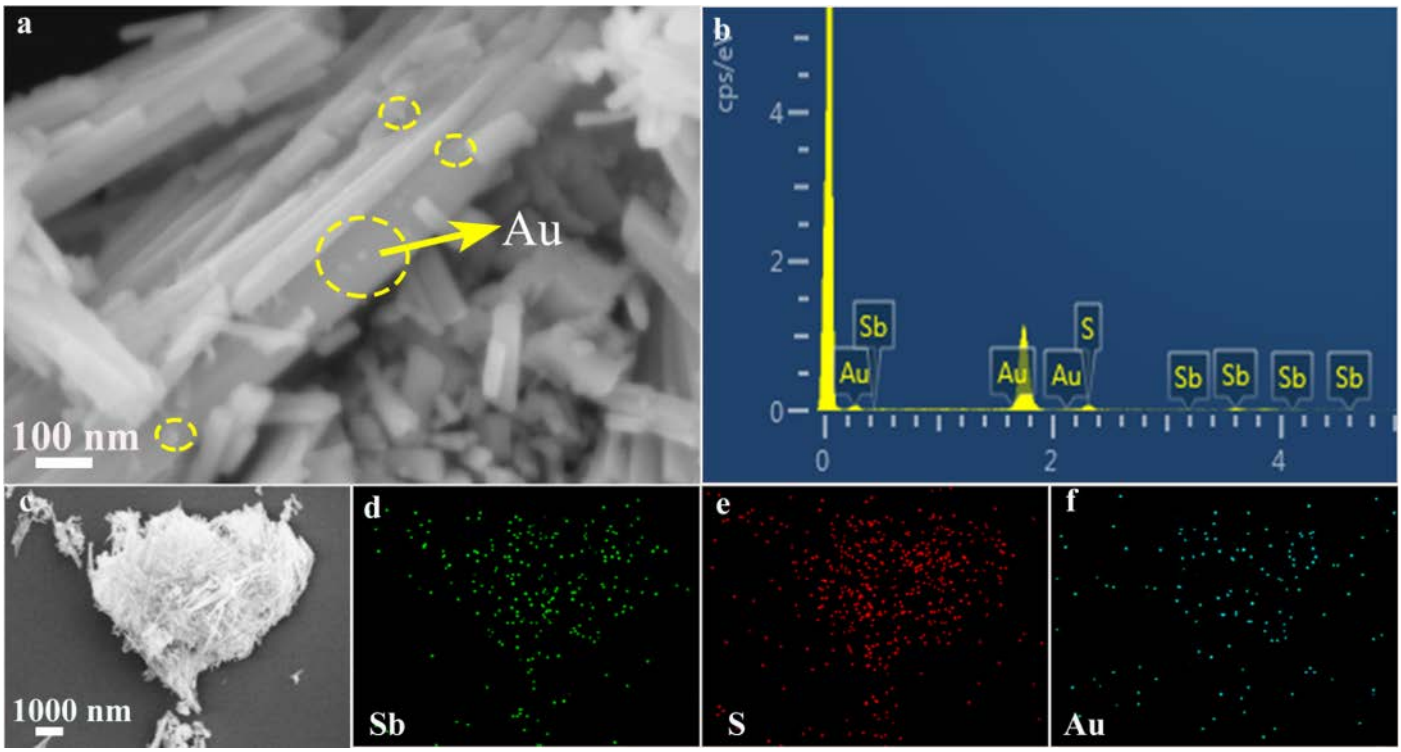

Fig. S6. SEM images (a) and EDX results (b) of Sb_2S_3 NRs-2%Au n heterostructure; elemental mapping results of Sb_2S_3 NRs-2%Au heterostructure for (d) Sb, (e) S and (f) Au signals.

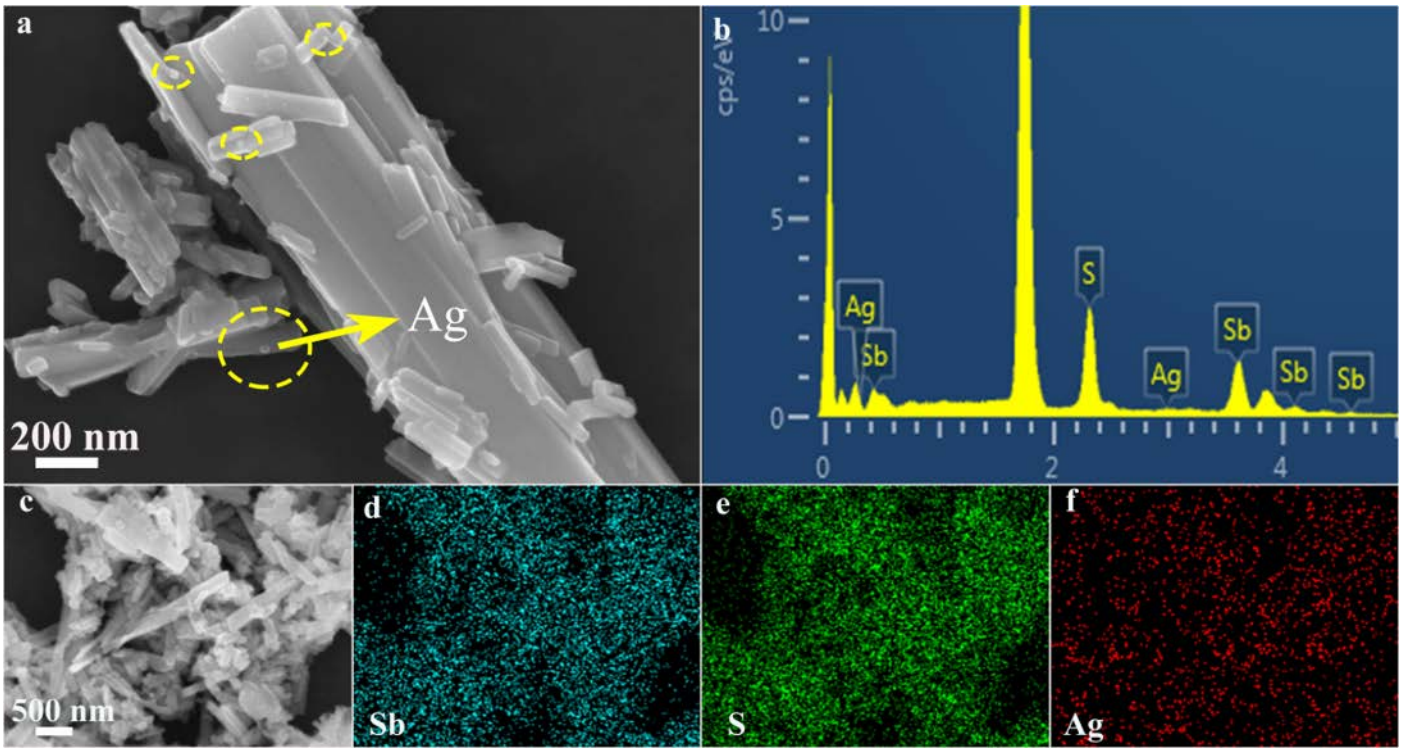

Fig. S7. (a & c) SEM images and (b) EDX results of Sb_2S_3 NRs-3%Ag heterostructure with elemental mapping results (d) Sb, (e) S and (f) Ag signals.

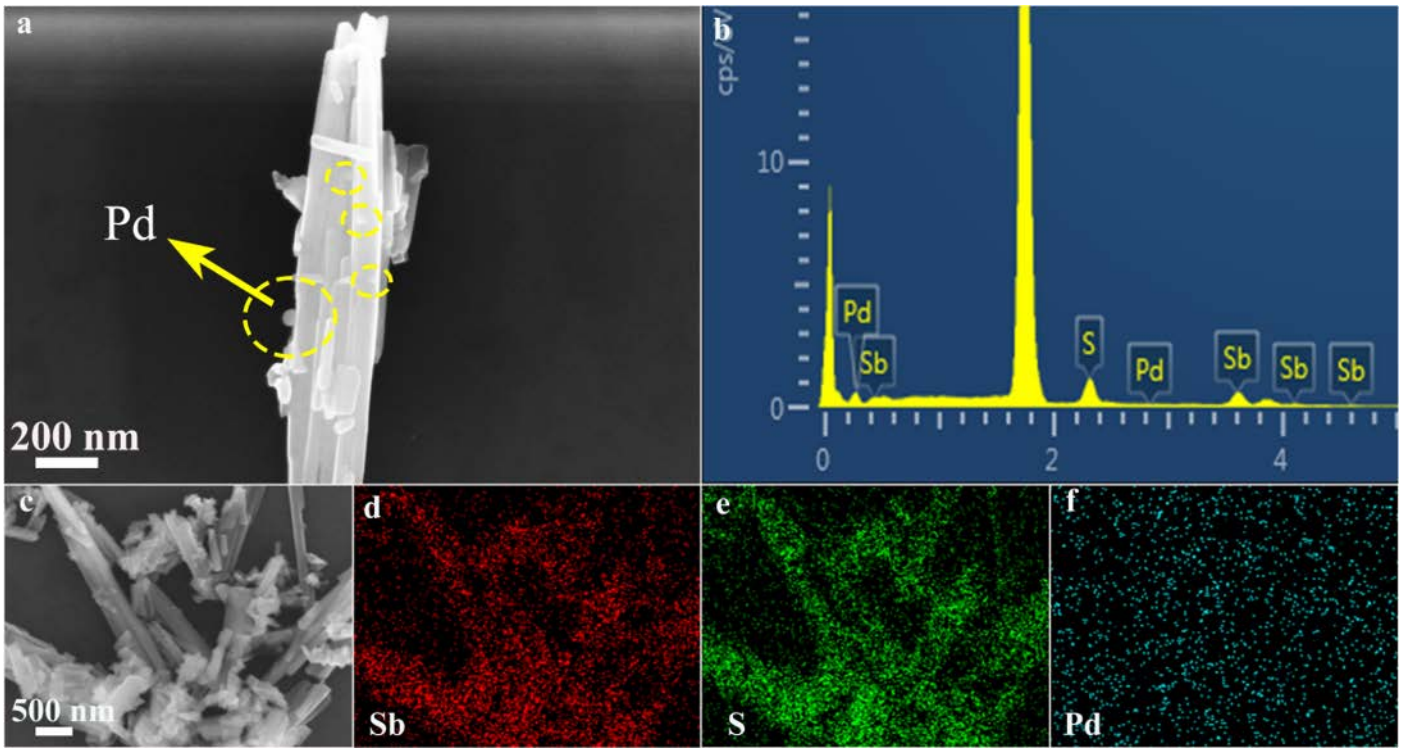

Fig. S8. (a & c) SEM images and (b) EDX result of Sb_2S_3 NRs-2%Pd heterostructure with elemental mapping results for (d) Sb, (e) S and (f) Pd signals.

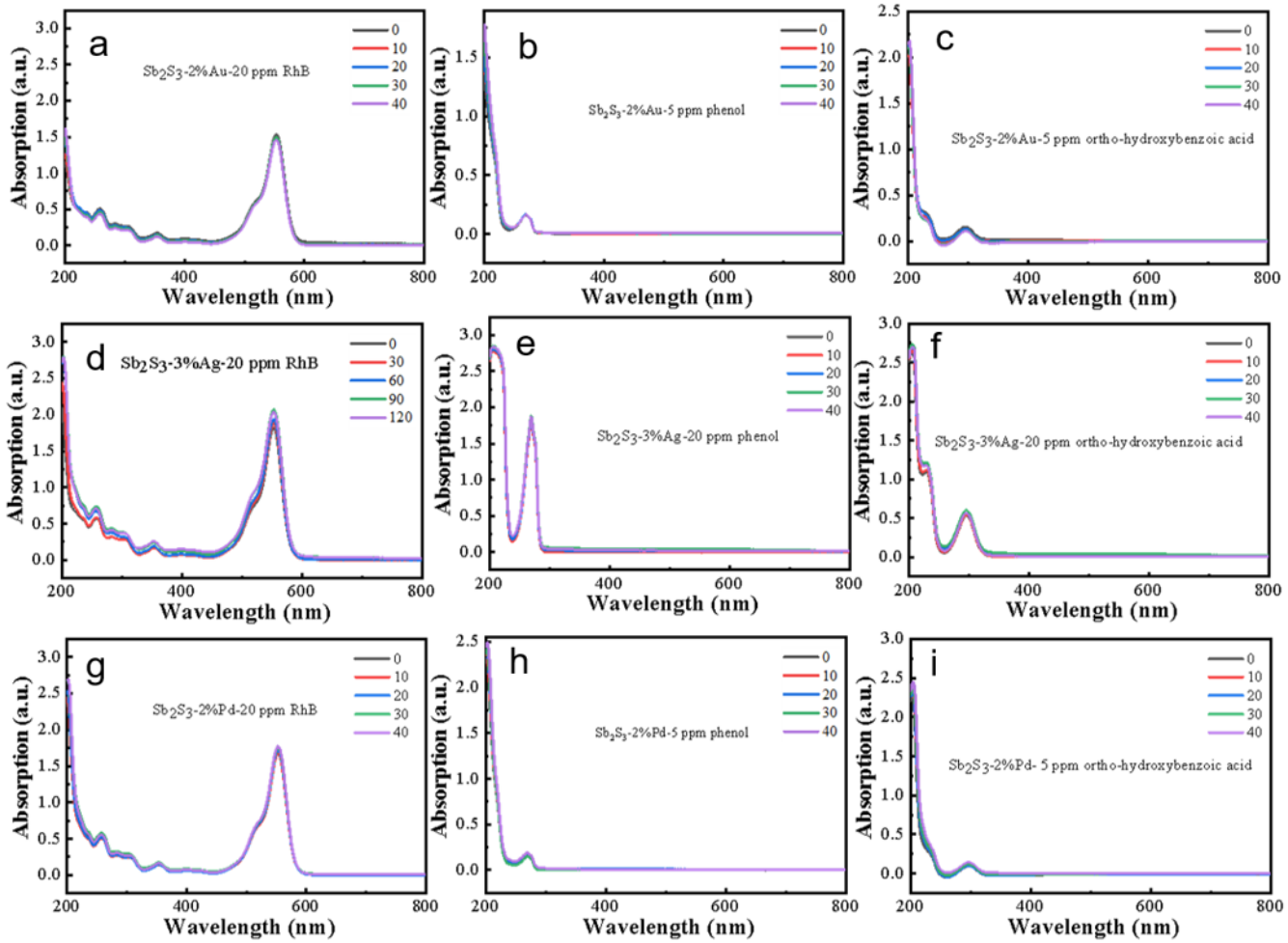

Fig. S9. Photoactivities of (a, b, c) Sb_2S_3 NRs-2%Au, (d, e, f) Sb_2S_3 NRs-3%Ag and (g, h, i) Sb_2S_3 NRs-2%Pd heterostructures toward degradation of RhB, phenol, and ortho-hydroxybenzoic acid under visible light irradiation (λ>420 nm), respectively.

Table S1. Chemical bond species vs. B.E. for different samples.

Element	Sb_2S_3 NRs	Sb_2S_3 NRs-2% Au	Sb_2S_3 NRs-3% Ag	Sb_2S_3 NRs-2% Pd	Chemical Bond Species
C 1s	284.6	284.6	284.6	284.6	C-C, C=C & C-H
Sb $3d_{5/2}$	529.6	529.6	529.6	530.0	Sb^{3+} [1,2]
Sb $3d_{3/2}$	539.0	539.0	539.0	539.4	Sb^{3+}
S $2p_{3/2}$	161.5	161.3	161.5	161.5	S^{2-} [1,2]
S $2p_{1/2}$	162.6	162.5	162.6	162.6	S^{2-}
Au $4f_{7/2}$	N.D.	84.1	N.D.	N.D.	Au^0 [3,4]
Au $4f_{5/2}$	N.D.	87.7	N.D.	N.D.	Au^0
Ag $3d_{5/2}$	N.D.	N.D.	368.2	N.D.	Ag^0 [5,6]
Ag $3d_{3/2}$	N.D.	N.D.	374.1	N.D.	Ag^0
Pd$3d_{5/2}$	N.D.	N.D.	N.D.	335.1	Pd^0 [7,8]
Pd $3d_{3/2}$	N.D.	N.D.	N.D.	340.3	Pd^0

N. D.: Not Detected.

Table S2. Peak positions along with the corresponding functional groups for blank Sb_2S_3 NRs, Sb_2S_3 NRs-2%Au, Sb_2S_3 NRs-3%Ag and Sb_2S_3 NRs-2%Pd heterostructures.

Peak position (cm^{-1})	**Vibration mode**
721	Sb-S
1365	COOH
1460	COOH
1650	COOH
2840	CH_2
2935	CH_2

Table S3. Summary of BET results for different results.

Samples	Specific Surface Area （m^2/g）	Pore Volume（cm^3/g）	Pore Size（nm）
Sb_2S_3 NRs	6.6711	0.008297	4.97501
Sb_2S_3 NRs-2% Au	11.4473	0.028025	9.7928
Sb_2S_3 NRs-3% Ag	9.4766	0.018194	7.67965
Sb_2S_3 NRs-2% Pd	29.3684	0.053209	7.24708

Table S4. Kinetic rate constants of Sb_2S_3 NRs-X%Au (X = 1, 2, 3, 4, 5) heterostructures toward degradation of MO visible light irradiation (λ>420 nm).

Kinetic rate (min^{-1})	Sb_2S_3 NRs	Sb_2S_3 NRs-1% Au	Sb_2S_3 NRs-2% Au	Sb_2S_3 NRs-3% Au	Sb_2S_3 NRs-4% Au	Sb_2S_3 NRs-5% Au
MO	0.0142	0.0269	0.0332	0.0145	0.0195	0.0270

Table S5. Kinetic rate constants of Sb_2S_3 NRs-X%Ag (X = 1, 2, 3, 4, 5) heterostructures toward degradation of MO under visible light irradiation (λ>420 nm).

Kinetic rate (min^{-1})	**Sb_2S_3 NRs**	**Sb_2S_3 NRs-1% Ag**	**Sb_2S_3 NRs-2% Ag**	**Sb_2S_3 NRs-3% Ag**	**Sb_2S_3 NRs-4% Ag**	**Sb_2S_3 NRs-5% Ag**
MO	0.0142	0.0138	0.0168	0.0186	0.0163	0.0153

Table S6. Kinetic rate constants of Sb_2S_3 NRs-X%Pd (X = 1, 2, 3, 4, 5) heterostructures toward degradation of MO under visible light irradiation (λ>420 nm).

Kinetic rate (min^{-1})	**Sb_2S_3 NRs**	**Sb_2S_3 NRs-1% Pd**	**Sb_2S_3 NRs-2% Pd**	**Sb_2S_3 NRs-3% Pd**	**Sb_2S_3 NRs-4% Pd**	**Sb_2S_3 NRs-5% Pd**
MO	0.0142	0.0343	0.0343	0.0318	0.0239	0.0245

References

1 H. L. Zhang, C. G. Hu, Y. Ding and Y. Lin, *J. Alloy. Compd.*, 2015, 625, 90-94.

2 X. Z. Yuan, H. Wang, J. J. Wang, G. M. Zeng, X. H. Chen, Z. B. Wu, L. B. Jiang, T. Xiong, J. Zhang and H. Wang, *Catal. Sci. Technol.*, 2018, 8, 1545-1554.

3 F.-X. Xiao, *J. Phys. Chem. C*, 2012, 116, 16487-16498.

4 Z. F. Bian, J. Zhu, F. L. Cao, Y. F. Lu and H. X. Li, *Chem. Commun.*, 2009, 25, 3789-3791.

5 Z. P. Zeng, F.-X. Xiao, H. Phan, S. F. Chen, Z. Z. Yu, R. Wang, T.-Q. Nguyen, T. T. Y. Tan, *J. Mater. Chem. A*, 2018, 6, 1700-1713.

6 Y. H. Zhang, Z. R. Tang, X. Z. Fu and Y. J. Xu, *Appl. Catal. B: Environ.*, 2011, 106, 445-452.

7 T. Li, Y.-B. Li, M.-H. Huang, X.-C. Dai, Y. H. He, G. C. Xiao and F.-X. Xiao, *J. Phys. Chem. C*, 2019, 123, 4701-4714.

8 H. Li, G. Chang, Y. Zhang, J. Tian, S. Liu, Y. Luo, A. M. Asiri, A. O. Al-Youbi and X. Sun, *Catal. Sci. Technol.*, 2012, 2, 1153-1156.